# EXPERIMENTAL PRESSURE AND HEAT TRANSFER INVESTIGATION OF A SPIKED BLUNT BODY AT MACH 10

**Paulo G.P Toro** - (toro@iae.cta.br)
Instituto de Aeronaútica e Espaço - IAE
Centro Técnico Aeroespacial - CTA - São José dos Campos - SP 12228-904 – BRAZIL
**Marco A.S. Minucci** - (sala@ieav.cta.br)
Instituto de Estudos Avançados - IEAv
Centro Técnico Aeroespacial - CTA - São José dos Campos - SP 12231-970 – BRAZIL
**Leik N. Myrabo** - (myrabl@rpi.edu)
**Henry T. Nagamatsu** - (nagamh@rpi.edu)
Department of Mechanical Engineering, Aeronautical Engineering, and Mechanics
Rensselaer Polytechnic Institute, Troy, NY 12180-3590 – USA

***Abstract.*** *The feasibility of transatmospheric flight is limited by phenomena such as aerodynamic drag and heating. For take off, escape from and flight through the earth's atmosphere the drag on the body should be reduced. For re-entry vehicle into the earth's atmosphere at a hypersonic speeds, it is important to have a large nose radius and high aerodynamic drag. An efficient hypersonic vehicle design has to combine a low drag coefficient with low heat transfer. A 6-in. diameter aluminum blunt body model was fabricated and fitted with pressure transducers and heat flux gauges over its forebody surface. A 6-in. long spike was placed at the stagnation point. Spiked blunt body with and without cooling gas flowing out of the spike were tested in the RPI 24-in. diameter Hypersonic Shock Tunnel. Freestream Mach 10 flow, with a stagnation temperature about 800 K, was selected to conduct the pressure and heat transfer measurements over the model. The spiked blunt body with and without cooling gas were very similar to each other. The measured pressure and heat transfer data indicate that the aerodynamic drag and heating of the spiked blunt body with cooling gas is lower than the aerodynamic drag and heating for the spiked blunt body without cooling gas. When the sonic cooling gas is injected through the physical spike; heat transfer over the model forebody surface decreases below that of the spiked blunt body with no cooling gas.*

**Key words:** spiked blunt body; hypersonic experimental investigation; pressure and heat transfer measurements.

## 1. INTRODUCTION

The feasibility of transatmospheric flight is limited by phenomena such as aerodynamic drag and heating, as well as related thermal management problems. Traditional blunt-nosed hypersonic vehicles generate a strong detached normal shock wave in the nose region, which produces high aerodynamic drag. The temperature behind this strong shock wave increases at hypersonic velocities, although the aerodynamic heating rates are reduced compared with that of an attached shock wave on a conical body. On the other hand, a traditional slender body with a sharp leading edge produces a conical weak attached shock wave with low drag coefficients, but extreme heating is created at the tip of the forebody.

To resolve these difficulties, an efficient transatmospheric hypersonic vehicle design has to combine a low drag coefficient (to maximize the net propulsive thrust) with low heat transfer rates (to minimize thermal protection system mass). One lightweight alternative to carry a sharp-nosed structural mass to induce conical shocks (Figure 1) that reduce aerodynamic drag and heating was proposed by using slender protruding spikes. [1-6]

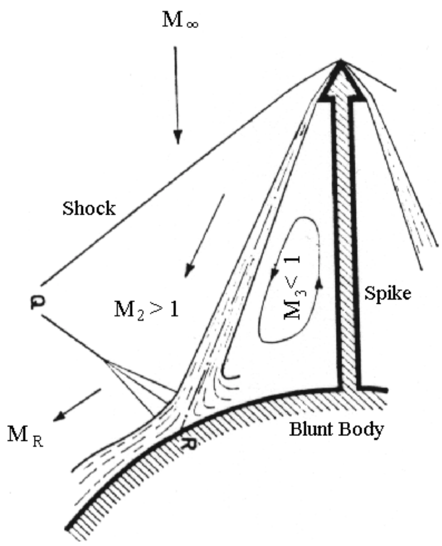

Figure 1 - Spiked blunt body phenomena.

Bogdonoff and Vas (1958, 1959) experimentally studied such flowfields around spiked (and unspiked) flat-faced and hemispherical-nosed axisymmetric bodies at a Mach number of about 14 in helium flow. They found that forebody pressure levels decreased by an order of magnitude and the heat transfer fell to a fraction of what it was without the spike. They also noted that an optimum spike length exists for minimum pressure on the hemisphere surface. They presented two techniques by which the heat transfer can possibly be reduced if the flow can be made to separate ahead of the blunt body and if the separated flow remains laminar. In this case, the drag and the heat transfer coefficients for the spiked blunt body were found to be lower than for the blunt body alone.

Crawford (1959) has confirmed the above observations. He also concluded that the physical spike reduces the drag-to-heat transfer ratio, thus compromising the use of such an artifact for reentry flight where a high drag-to-heat ratio is necessary. Subsequent investigations explained in detail the reattachment process as well as the oscillatory type of flow behavior on spiked axisymmetric bodies at Mach 6.8, and spiked cone-cylinders at Mach 10.

The reattachment point, defined as the intersection of the spike-induced shear layer and the blunt body surface (Figure 1), impinges the shoulder of a spike-fitted blunt body, the drag should be a minimum. However, Wood (1962) asserts that the shoulder radius of a given blunt body influences whether the reattachment point impinges the body or not. In addition, he states that the body shoulder plays an active role in drag reduction, since the presence of the shoulder induces expansion waves which propagate upstream of the reattachment point. The pressure rises at that location and decreases as the reattachment point approaches the body shoulder. This is to be expected since the reattachment point is associated with a localized high pressure area. When this point is located at a surface which is normal or nearly perpendicular to the body axis, then the component of pressure along the symmetry axis (i.e., the drag direction) will be minimized.

Maull (1960) experimentally investigated the flow over axisymmetric spiked bodies at a Mach number of 6.8 and Reynolds number of $0.17 \times 10^6$/in. For some ranges of the ratio of spike length to body diameter, the flow was found to be unsteady. The effect of the shape of the body nose on this unsteadiness was investigated as well, and an explanation of the mechanism of the oscillation was given.

An experimental evaluation of the oscillations on spiked protruded surfaces was recently addressed by Calarese et al. (1985). For some spike lengths, the shock oscillations are symmetric. For other spike lengths, the shock structure oscillates asymmetrically, with respect to the spike's axis. In this case, experimental evidence confirms the presence of standing rotational waves on the body face and spike. Spike configurations resulting in stable shock systems are also observed.

For spike-attached-hemispheres in hypersonic Mach 7 flow, the effect of the length and nose configuration on the reduction of pressure drag was investigated, by Kubota et al (1994) in both wind tunnel experiments and numerical simulations (Navier-Stokes using the TVD approach). The pressure distributions over the hemisphere are influenced significantly by the spike length and nose configuration. The pressure drag is further reduced by increasing the spike length and by using a hemispherical, rather than a conical nose spike.

Fujita and Kubota (1992) have numerically investigated the hypersonic flowfield over a hemisphere equipped with a spike at the stagnation point by solving the axisymmetric, compressible Navier-Stokes equations using TVD difference and Runge-Kutta methods. The results obtained for Mach 6.8 and Reynolds number of $1.2 \times 10^5$ agree quantitatively with the existing experimental data. Recently, Yamauchi et al. (1995) numerically simulated the supersonic flow over a spiked blunt body and found that the drag was reduced, compared to the blunt body with no spike. These above numerical researchers characterized the flowfield by 1) a conical attached shock wave from the tip of the spike, 2) a separated region in front of the blunt body, air-dead region, and 3) the resulting reattachment shock wave (Figure 1).

The present model of the spike with gas flowing inside the spike, will produce a flowfield which is formed by exhausting an underexpanded sonic jet in a direction opposite to that of the hypersonic mainstream (Figure 2).

The flowfield of the sonic jet, as studied by Moraes and Ganzer (1985) and Moraes (1987) is complex and presents very large gradients of the flow properties. It is well characterized by 1) the formation of a bow shock wave in the mainstream; 2) a curved shock wave in the jet flow; 3) an approximately semi-spherical contact surface between both flow components; 4) a dead-air region in front of the jet nozzle; and 5) some other discontinuities (Figure 2). Such flowfields may be found for instance in: 1) nose cooling systems for thermal protection of re-entry bodies; 2) supersonic combustion systems; 3) retro-rocket systems, and; 4) secondary injection systems for thrust vector control. The pressure distribution indicates that the jet works as an *aerodynamic spike* (in analogy to a spike without cooling gas). It produces a reduction of the static pressure on the body front surface by inducing a flow separation, and so reduces the overall drag of that body due to reduced dynamic pressure in the separated flow.

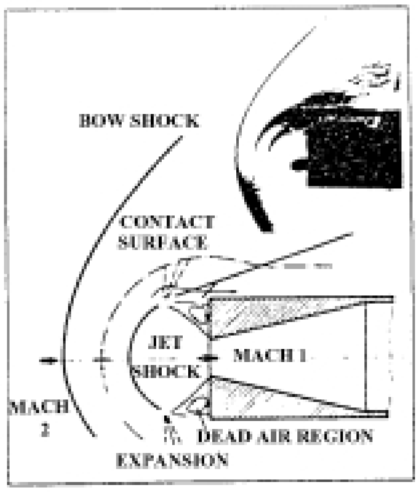


Figure 2 - Supersonic counter-flow.

## 2. EXPERIMENTAL APPARATUS

The design of a transatmospheric vehicle using spiked blunt body with sonic cooling gas through the spike presents the following advantage (Figure 3); it employs a detached conical (parabolic-shaped) shock wave to contain a hot air pocket which substantially reduces the flow Mach number impacting the vehicle forebody, and consequently decreases the aerodynamic drag and heating compared with the spiked blunt body without cooling gas.

A 6-in. diameter aluminum model, “double Apollo disc”, scaled from the Apollo Command Module’s lower heat shield, was fabricated and instrumented with piezoelectric pressure transducers and thin-film platinum heat gauges. The “double Apollo disc” model was equipped with a 6-in. long slender spike, located at the stagnation point. The experimental investigation was conducted, by Toro (1998), in the RPI 24-in. diameter Hypersonic Shock Tunnel, at freestream Mach 10 flow with stagnation temperature of about 800K.

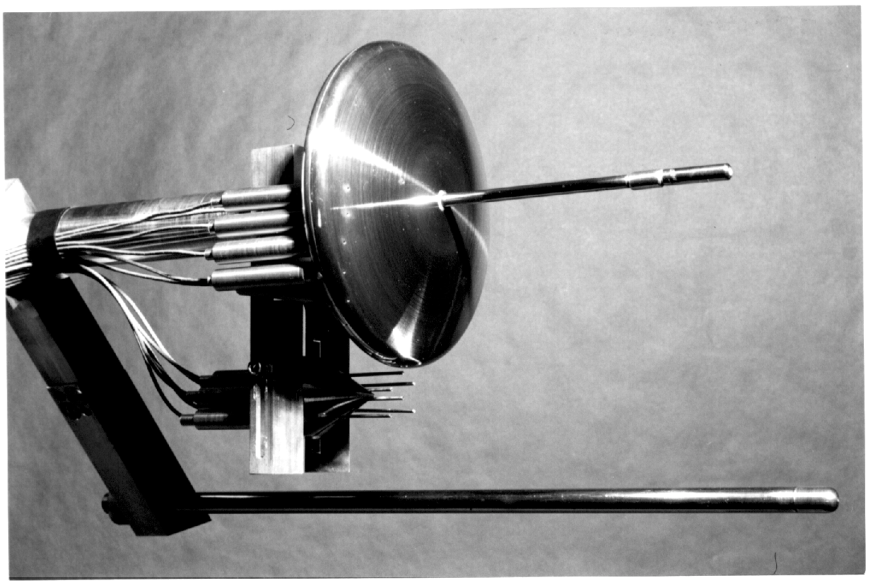

Figure 3 - “double Apollo disc” model equipped with the spiked and pressure transducers.

Note that when the spike (with no cooling gas) is joined with the disk shaped model, the result is simply a spiked blunt body (Figure 1) in hypersonic flow. The central stagnation point of the Lightcraft model was fitted with an spike measuring 6-in. long and 0.25-in. external diameter. The spike is fitted with an axial tungsten and a cylindrical copper tip. The spike is designed for a choked (i.e., sonic orifice) airflow existing at the tip, in order to simulate the counter flow during the hypersonic test.

The short test time of the RPI Hypersonic Shock Tunnel, on the order of a few milliseconds, requires the development of fast response heat flux sensors. Thin-film platinum heat gauges are specially suited for use in shock tubes and shock tunnels. Small diameter (2.4 to 3.4 mm) thin-film platinum heat transfer gauges were designed, developed, and constructed to measure the voltage changes when installed on the model. Pyrex and Macor materials were used as a substrate for the thin-film. The RPI 4-in. diameter Low Pressure Shock Tube was used to dynamically calibrate the thin-film platinum heat gauges.

## 3. RPI 24-in. diameter HYPERSONIC SHOCK TUNNEL

The RPI 24-in. diameter Hypersonic Shock Tunnel is capable of producing test section Mach numbers ranging from 8 to 25, with stagnation temperature and pressure up to 4100 K and 1500 psi, respectively. The useful test times is about 3 to 6 milliseconds, enough time to obtain the aerodynamic parameters such as pressure and heat flux distributions. The facility was used to obtain the Mach number 10 flow for the present experiment with a stagnation temperature about 800 K.

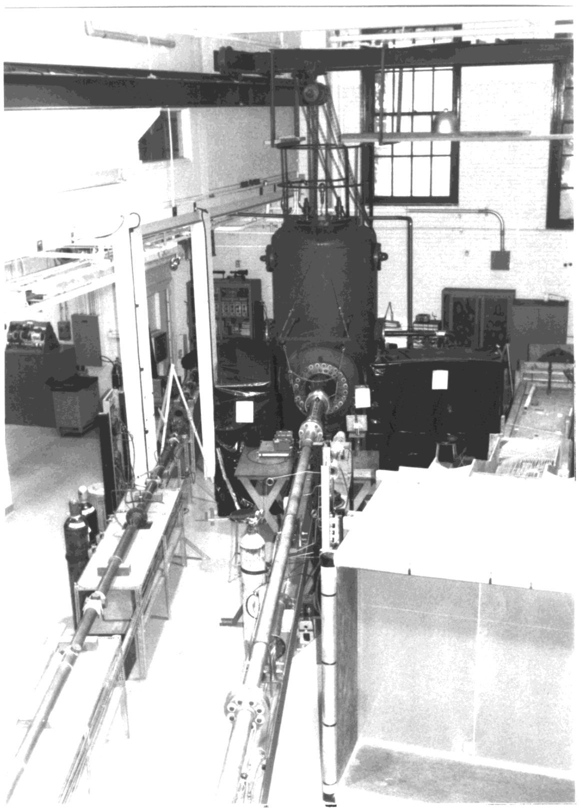

Figure 4 - RPI 24-in. diameter Hypersonic Shock Tunnel.

## 4. EXPERIMENTAL RESULTS AND DISCUSSION

When the blunt body model is fitted with the spike and no cooling gas flow out of the spike tip the flowfield (Figure 5), the result is very similar to the well-known spiked blunt body experiments (Figure 1). The Schlieren photograph (Figure 5) reveals the location of the shear layer reattachment point, and the conical shape of the shock wave.

Under the influence of the nearly normal shock wave in front of the spike's tip, the flow separates near to the corner of the tip (Figure 6) and the shear layer reattaches on the blunt body surface (Figure 5) enclosing an approximately conical region between the conical shock wave and the blunt body surface. The interaction between the shear layer on the model surface causes the second separation flow, near the reattachment point. The conical region contains a circulatory, dead-air flow, with low pressure ratio, due to the decrease in pressure across the conical shock wave. For the nearly flat-hemispherically-nosed bodies with rounded shoulders, there will be a shear layer reattachment point where the pressure ratio across the conical shock is just sufficient for equilibrium of the recirculation air region, and no oscillation occurs.

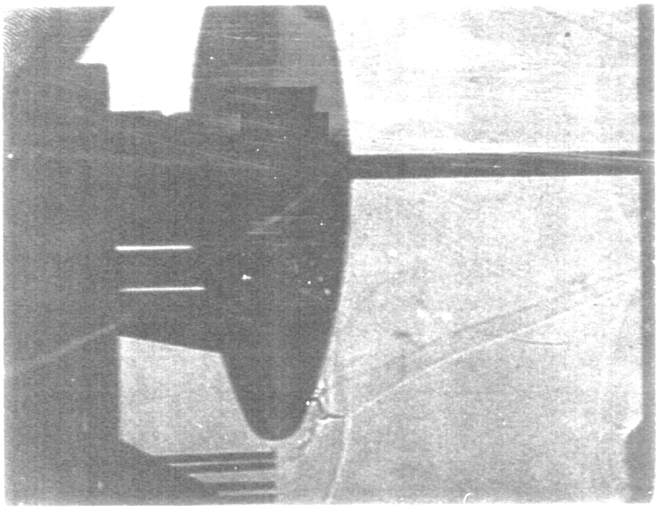

Figure 5 - Schlieren photograph of the spiked blunt body without gas.

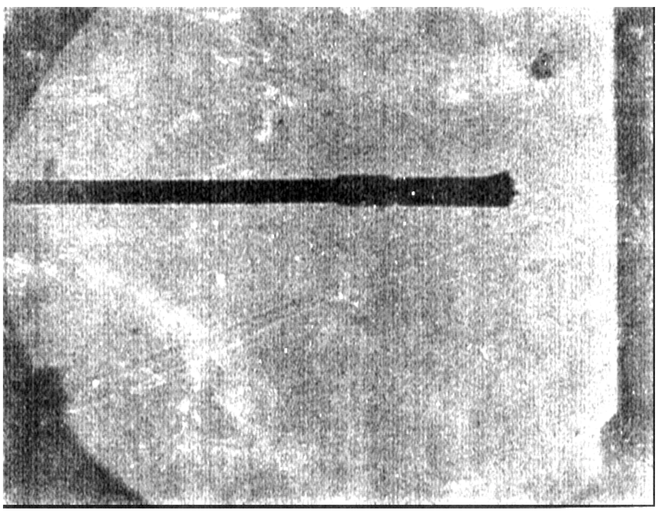

Figure 6 - Schlieren photograph at the tip of the spiked blunt body without gas.

When mass is injected through the spike, the incident flowfield is formed by exhausting an underexpanded sonic jet in a direction opposite to that of the hypersonic flow (Figure 2). In the present investigation, no Schlieren photograph was obtained of the flowfield at the spike tip with gas through the spike. Moraes and Ganzer (1985) and Moraes (1987) experimentally investigated the flowfield of a sonic jet exhausting against a supersonic mainstream but without any solid body behind it; hence there could be no interaction between the shear layer/conical shock wave and the body surface. Also, no available literature exists on the spiked blunt body with a sonic jet out the spike in a direction opposite to the main hypersonic flow. Nevertheless, the sonic jet flowfield should be characterized by the formation of a bow shock wave in the hypersonic freestream flow, a curved shock wave in the jet flow, an approximately semi-spherical contact surface between both flow components, a dead-air flow region in front of the jet nozzle and some other discontinuities (Figure 2).

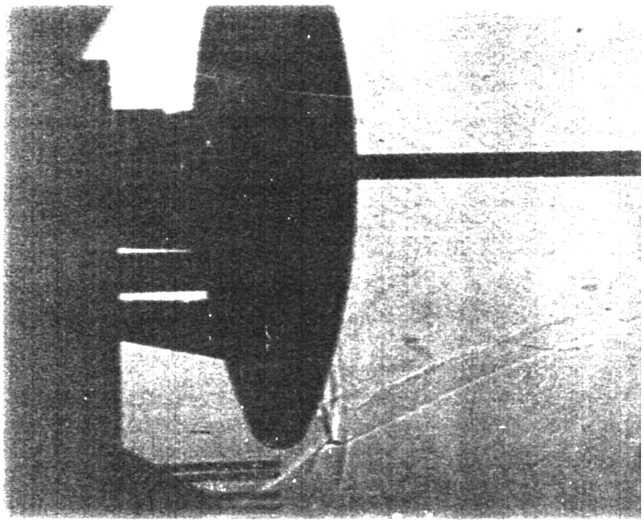

Figure 7 - Schlieren photograph for spiked blunt body with sonic cooling gas flow out the spike.

The Schlieren photograph (Figure 7) shows not only the location of the shear layer reattachment point, but also the complex geometry of the first and the second conical shock wave structures. After comparing both Schlieren photographs, spiked blunt body without gas out the spike (Figure 7) and spiked blunt body with gas through the spike (Figure 7) one may conclude the following: the thickness of the compressed air region between the shear layer and the shock wave increases as mass is injected through the spike. Consequently, the shear layer moves towards the recirculation, dead-air region.

Experimental pressure ratio results for the spiked blunt body surface at Mach 10 (Figure 8) indicate that the pressure at the shear layer reattachment point is maximum. Figure 8 also shows a reduction of the pressure ratio across the second conical shock wave, at the corner, between the shear layer and the shock wave. When mass is injected through the spike, the maximum pressure ratio at the shear layer reattachment point decreases. This result agrees with Moraes' (1985, 1987) experimental results for the sonic flow against the freestream supersonic flow. The pressure ratio increases at the inner recirculation region, r/R=0.8333 (Figure 8).

Drag is due both to the pressure and shear stress distributions. Since the shear stress distribution was not measured, the drag force is calculated using the pressure distribution only. The pressure drag coefficient is calculated by the following equation

$$c_D = \frac{\int_{S_i}^{S_f} p dS}{\frac{1}{2}\rho_\infty U_\infty^2 S}$$

where S is the cross-sectional area of the blunt body model, $\rho_\infty$ and $U_\infty$ are the free stream density and the free stream velocity, respectively.

The experimental drag coefficient using the surface pressure distributions for Mach 10 flow and stagnation temperature of 800 K for the spiked blunt body with and without sonic cooling gas are about 0.74 and 0.84, respectively. In agreement with the pressure ratio measurements (Figure 8) and the Schlieren photographs (Figures 5 and 7) the aerodynamic drag for the case of sonic cooling gas flowing out of the spike is smaller than that of the spiked blunt body without cooling gas configuration.

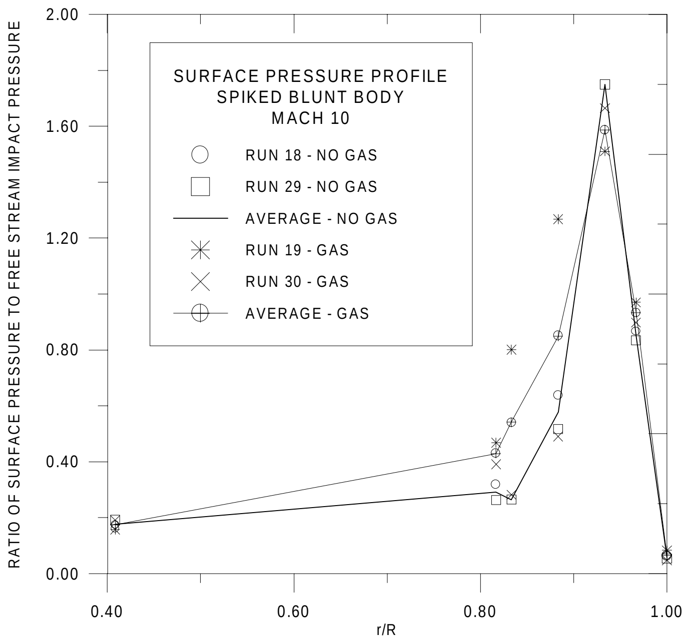


Figure 8- Pressure ratio for spiked blunt body with and without cooling gas

When the sonic cooling gas is injected through the spike, the heat transfer over the model surface decreases compared with the case of the spiked blunt body with no cooling gas. The physical explanation for this result is that the low temperature and thermal mass of the sonic cooling gas emerging from the spike tip. Of a period of approximately 20 ms, about 0.15 to 0.20 g/s of cooling air is injected at ambient temperature. This flow rate out the spike tip of sonic cooling gas is enough to cool down the flow inside the conical shock wave (Figure 9).

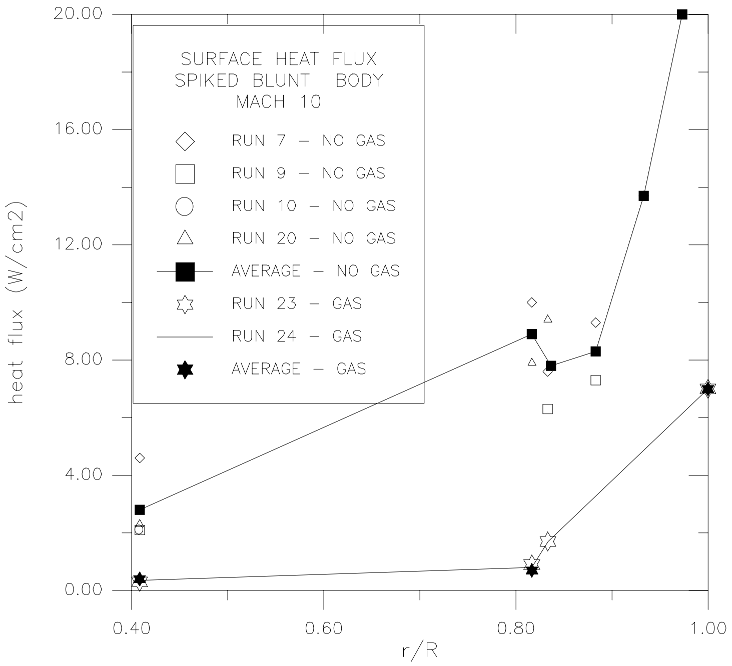

Figure 9 - Heat flux for spiked blunt body with and without cooling gas.

## 5. CONCLUSIONS

The primary objective of the present experimental investigation was to provide experimental data required for understanding the hypersonic flow characteristics over a Double Apollo disc with Air Spike for an advanced transatmospheric vehicle.

A 6-in. diameter aluminum model, scaled from the Apollo Command Module's lower heat shield, was fabricated and instrumented with pressure transducers and heat transfer gauges. The model was equipped with a 6-in. long slender spike, located at the stagnation point.

The experimental investigation was conducted in the RPI 24-in. diameter Hypersonic Shock Tunnel on the following distinct model configurations: spiked blunt body with no cooling gas and spiked blunt body with sonic cooling gas flowing in a direction opposite that of the freestream hypersonic flow. Freestream Mach number 10 flow with stagnation temperature of 800K was selected to conduct the pressure and heat transfer measurements over the model.

Schlieren photographs were taken to provide flow visualization for the complex conical shock wave structure and shear layer. Schlieren photographs reveal that when a freestream hypersonic Mach number of 10 is established over the model with spiked (with and without sonic cooling gas), the flowfield is very similar to the known spiked blunt body experiments.

Small diameter (2.4 to 3.4 mm) thin-film platinum heat transfer gauges were designed, developed, and constructed to measure the voltage changes when installed on the model. Pyrex and Macor materials were used as a substrate for the thin-film.

The measured pressure and heat transfer data indicate that the aerodynamic drag and heating of the spiked blunt body with cooling gas is lower than the aerodynamic drag and heating for the spiked blunt body without cooling gas.

The experimental measured heat transfer on the present blunt body, with no cooling gas, arises on the corner region. However, the maximum heat transfer occurs aft of the shear reattachment point, probably due to the rapid flow expansion at the corner. When the sonic cooling gas is injected through the physical spike; heat transfer over the model forebody surface decreases below that of the spiked blunt body with no cooling gas. Evidently, the flow rate of sonic cooling gas is sufficient to cool down the air momentarily trapped inside the conical shock wave.

## ACKNOWLEDGMENTS

This report was prepared under contract no. NCC8-112 for NASA Marshall Space Flight Center. The first author wishes to thank the Brazilian Foundation (FAPESP) for supporting his graduate studies, and the Aeronautic and Space Institute (IAE) which allowed him to pursue graduate studies at Rensselaer Polytechnic Institute (RPI).

## 6. LITERATURE CITED

Bogdonoff, S. M. and Vas, I. E. "Preliminary Investigations of Spiked Bodies at Hypersonic Speeds," J. of AeroSpace Sciences, Vol. 26, No.2, pp. 65-74, Feb. 1959.

Bogdonoff, S. M. and Vas, I. E. "Exploratory studies of a Spiked Body for Hypersonic Flight," Gas Dynamics Laboratory, Princeton University, Mar. 1958.

Calarese, W. and Hankey, W. L. "Modes of Shock-Wave Oscillations on Spiked-Tipped Bodies," AIAA Journal, Vol. 23, No. 2, pp. 185-192, Feb. 1985.

Crawford, D. "Investigation of the Flow over a Spiked-Nose Hemisphere-Cylinder," NASA TN D-118, December, 1959.

Fujita, M. and Kubota, H. "Numerical Simulation of Flowfield over a Spiked Blunt-Nose," Computational Fluid Dynamics Journal, Vol. 1, No. 2, July 1992,pp. 187-195.

Kubota, H., Watanulci, T., Matsumoto, S., Fujita, M. "Effect of Spike Attached on a Hemisphere in Hypersonic Flow," Proceedings of the 19th International Symposium on Space Technology, and Science, Yokohama, 1994, pp. 363-369.

Maull, D. "Hypersonic Flow over Axially Symmetric Spiked Bodies," J. of Fluid Mechanics, Vol. 8, No. 4, pp. 584-592, 1960.

Moraes Jr., P. and Ganzer, U. "The Flowfield of a Sonic Jet Exhausting against a Supersonic Flow," VIII COBEM, pp. 113- 115, Brazil, Dec. 1985.

Moraes Jr., P. "Pressure Measurements in a Supersonic Counter-Flow," IX COBEM, Brazil, Dec. 1987.

Toro, P.G.P., "Experimental and Heat Transfer Investigation over a "Directed_Energy Air Spike" Inlet at Flow Mach Numbers 10 to 20, Stagnation Temperature of 1000K, and Arc Power up to 127 KW," Ph.D. Thesis, Rensselaer Polytechnic Institute, June 1998.

Yamauchi, M., Fujii, K., and Higashino, F. "Numerical Investigation of Supersonic Flows Around a Spiked Blunt Body," J. of Spacecraft and Rockets, vol. 32, no. 1, Jan./Feb. 1955.

Wood, C. "Hypersonic Flow over Spiked Cones," J. of Fluid Mechanics, Vol. 12, No. 4, pp. 614-624, 1962.